Myelin quantification with MRI

van der Weijden, Chris W J; Vállez García, David; Borra, Ronald J H; Thurner, Patrick; Meilof, Jan F; van Laar, Peter-Jan; Dierckx, Prof Rudi A J O; Gutmann, Ingomar W; de Vries, Erik F J

Published in:
Neuroimage

DOI:
10.1016/j.neuroimage.2020.117561

NeuroImage 226 (2021) 117561

Contents lists available at ScienceDirect

NeuroImage

journal homepage: www.elsevier.com/locate/neuroimage

Myelin quantification with MRI: A systematic review of accuracy and reproducibility

Chris W.J. van der Weijden[a], David Vállez García[a,b], Ronald J.H. Borra[b], Patrick Thurner[c], Jan F. Meilof[d], Peter-Jan van Laar[b,e], Rudi A.J.O. Dierckx[a], Ingomar W. Gutmann[f], Erik F.J. de Vries[a,*]

[a] Department of Nuclear Medicine and Molecular Imaging, University of Groningen, University Medical Center Groningen, Hanzeplein 1, 9713 GZ Groningen, the Netherlands
[b] Department of Radiology, University of Groningen, University Medical Center Groningen, Hanzeplein 1, 9713 GZ Groningen, the Netherlands
[c] Universitätsklinik für Radiologie und Nuklearmedizin, Medizinische Universität Wien, Währinger Gürtel 18-20, 1090 Wien, Austria
[d] Multiple Sclerosis Center Noord Nederland, University of Groningen, University Medical Center Groningen, Hanzeplein 1, 9713 GZ Groningen, the Netherlands
[e] Department of Radiology, Zorggroep Twente, Zilvermeeuw 1, 7609 PP Almelo, the Netherlands
[f] Physics of Functional Material, Faculty of Physics, University of Vienna, Boltzmanngasse 5, 1090 Vienna, Austria

ARTICLE INFO

Keywords:
Myelin sheath
Magnetic resonance imaging
Multiple sclerosis
Demyelinating diseases
Neurodegenerative diseases

ABSTRACT

Objectives: Currently, multiple sclerosis is treated with anti-inflammatory therapies, but these treatments lack efficacy in progressive disease. New treatment strategies aim to repair myelin damage and efficacy evaluation of such new therapies would benefit from validated myelin imaging techniques. Several MRI methods for quantification of myelin density are available now. This systematic review aims to analyse the performance of these MRI methods.

Methods: Studies comparing myelin quantification by MRI with histology, the current gold standard, or assessing reproducibility were retrieved from PubMed/MEDLINE and Embase (until December 2019). Included studies assessed both myelin histology and MRI quantitatively. Correlation or variance measurements were extracted from the studies. Non-parametric tests were used to analyse differences in study methodologies.

Results: The search yielded 1348 unique articles. Twenty-two animal studies and 13 human studies correlated myelin MRI with histology. Eighteen clinical studies analysed the reproducibility. Overall bias risk was low or unclear. All MRI methods performed comparably, with a mean correlation between MRI and histology of R^2=0.54 (SD=0.30) for animal studies, and R^2=0.54 (SD=0.18) for human studies. Reproducibility for the MRI methods was good (ICC=0.75–0.93, R^2=0.90–0.98, COV=1.3–27%), except for MTR (ICC=0.05–0.51).

Conclusions: Overall, MRI-based myelin imaging methods show a fairly good correlation with histology and a good reproducibility. However, the amount of validation data is too limited and the variability in performance between studies is too large to select the optimal MRI method for myelin quantification yet.

List of abbreviations

- COV Coefficient Of Variance.
- ICC Intraclass Correlation Coefficient.
- ihMTR inhomogeneous Magnetization Transfer Ratio.
- MBP Myelin Basic Protein.
- mcDESPOT multicomponent Driven Equilibrium Single Pulse Observation of T1 and T2.
- MS Multiple Sclerosis.
- MTR Magnetization Transfer Ratio.
- MWF Myelin Water Fraction.
- PGSE Pulsed Gradient Spin Echo.
- PLP ProteoLipo Protein.
- qihMT quantitative inhomogeneous Magnetization Transfer.
- qMT quantitative Magnetization Transfer.
- QSM Quantitative Susceptibility Mapping.

* Corresponding author.
E-mail addresses: c.w.j.van.der.weijden@umcg.nl (C.W.J. van der Weijden), d.vallez-garcia@umcg.nl (D.V. García), r.j.h.borra@umcg.nl (R.J.H. Borra), patrick.thurner@meduniwien.ac.at (P. Thurner), j.f.meilof@umcg.nl (J.F. Meilof), p.j.van.laar@umcg.nl, p.vlaar@zgt.nl (P.-J. van Laar), r.a.dierckx@umcg.nl (R.A.J.O. Dierckx), ingomar.gutmann@univie.ac.at (I.W. Gutmann), e.f.j.de.vries@umcg.nl (E.F.J. de Vries).

https://doi.org/10.1016/j.neuroimage.2020.117561
Received 27 May 2020; Received in revised form 27 October 2020; Accepted 7 November 2020
Available online 12 November 2020

- QUADAS Quality Assessment of Diagnostic Accuracy Studies.
- SyMRI Synthetic MRI.
- UTE Ultrashort Echo Time.

1. Introduction

Multiple sclerosis (MS) is the most common neurodegenerative disease in young adults (Ramagopalan et al., 2010). MS pathology is characterized by inflammatory, demyelinated lesions in the central nervous system (CNS). These lesions can be detected with magnetic resonance imaging (MRI). Thus, MRI can support MS diagnosis and show disease progression. However, MRI abnormalities in CNS lesions can originate from multiple factors like inflammation, demyelination, axonal loss, and gliosis, and are thus not specific for evaluating a single biological process (Brück et al., 1997; Wayne Moore, 2003). Current treatment of MS is mainly focused on suppressing inflammation in the lesions and thereby decreasing further myelin damage. However, anti-inflammatory treatment has not been able to cure or stop the progression of MS so far.

New treatments for MS are being developed that do not target inflammation, but aim to stimulate myelin repair. Myelin is a fatty substance that forms a protective layer around axons and enhances axonal conductance. Myelin damage can cause axonal dysfunction, resulting in a wide variety of neurological symptoms (Alizadeh et al., 2015). For assessment of efficacy of these new myelin repair treatments, accurate *in-vivo* quantification of myelin is needed. Until now, several MRI methods have been developed for the quantification of myelin density (see Heath and colleagues, 2017 (Heath et al., 2017) for a thorough explanation). To validate these MRI methods as tools for assessment of myelin density, the methods should be evaluated against the current gold standard for myelin quantification, i.e. histology. Subsequently, a verdict on the specificity, accuracy and reproducibility of these MRI measurements has to be reached.

This review aims to evaluate the performance of the current MRI methods for myelin quantification in both animals and humans by assessing the correspondence of the MRI measures with myelin histology data, and their reproducibility. The evaluated myelin MRI methods are T1 mapping (hereafter referred to as T1), T2 mapping (hereafter referred to as T2), T1w/T2w ratio, Myelin Water Fraction (MWF), R2*, Quantitative Susceptibility Mapping (QSM), multicomponent Driven Equilibrium Single Pulse Observation of T1 and T2 (mcDESPOT), Magnetization Transfer Ratio (MTR), quantitative Magnetization Transfer (qMT), inhomogeneous Magnetization Transfer Ratio (ihMTR), quantitative inhomogeneous Magnetization Transfer (qihMT), Synthetic MRI (SyMRI), Ultrashort Echo Time (UTE), and g-ratio.

2. Methods

2.1. Search & selection procedure

This systematic review was conducted in accordance with the PRISMA-DTA statement, according to the recommendations of McInnes and Bossuyt, and McGrath and colleagues (McGrath et al., 2019; McInnes et al., 2018; McInnes and Bossuyt, 2015). PubMed/MEDLINE and Embase were searched for studies on myelin MRI published until December 2019, using the search strings shown in the Appendix, without language restrictions. Retrieved studies were assessed by two authors. Studies describing MRI methods for quantification of myelin density were included if they quantitatively assessed either the correspondence of MRI results with myelin histology in the same subject, or the reproducibility of the MRI method. Any study assessing myelin MRI was considered irrespective of studied pathogenesis, since the efficacy of a method should be independent of the studied disease. Studies that contained only *in-vitro,* or simulated data and studies that lacked quantitative measurements were excluded. While diffusion MRI has been used as a marker for myelin integrity, it is becoming common knowledge that the long acquisition TEs of diffusion MRI makes it insensitive for myelin, which has a short T2 (MacKay and Laule, 2016; Varma et al., 2015). In addition, diffusion MRI is not capable of differentiating between axonal or myelin damage. Because the differentiation is an essential aspect for the evaluation of the efficacy of remyelination therapies, we excluded studies correlating diffusion MRI with myelin histology.

2.2. Risk of bias assessment

The Quality Assessment of Diagnostic Accuracy Studies (QUADAS)-2 tool was used to assess the risk of bias in the correlation between MRI and histology, and the reproducibility assessment by two authors (Whiting et al., 2011). The QUADAS-2 tool assesses four key domains: patient/sample selection, index test, reference standard, and flow-and-timing. For this study, the index test was the MRI method and the reference standard was myelin histology. The bias assessment for the reproducibility studies comprised the same methodology as used for the histological studies, but excluding the reference standard in the QUADAS-2 tool. Risk of bias was scored for each domain as low, unclear, or high. The total risk of bias judgment was based on the assessment of all domains and the overall quality of the paper.

2.3. Data analysis

All studies correlating MRI results with myelin histology used either R or R^2 values to describe the correspondence. If necessary, R values were converted to R^2 values. Sample size weighted mean R^2 values, based on the number of subjects in each study, were calculated per MRI method and over all studies. Due to the absence of a normal distribution of the data, the influence of the use of *ex-vivo* or *in-vivo* MRI, the use of fresh or fixated CNS samples, and the histological method to quantify myelin was individually assessed with the Mann Whitney U test and the Kruskal Wallis test (non-parametric equivalents for the t-test and ANOVA, respectively), using IBM SPSS statistics 23, without correction for multiple comparisons. The Mann Withney U test, generates an U value that can range from 0 to the product of the number of subjects in each group (n1*n2), with a bigger U value indicating less difference between groups. The Kruskal Wallis test generates an H as test statistic, with higher H values, indicating more difference between groups. Differences were considered statistically significant if the probability (p) was <0.05. Forest plot analysis was performed for myelin histological correspondence with MRI for both animal and human studies.

For reproducibility assessment, any measure of variance was extracted. R^2 values, Intraclass Correlation Coefficient (ICC), Coefficient Of Variance (COV), and similarity were used as measures of variance. R^2 and ICC values can range between 0 and 1: the closer the reported value is to 1, the higher the degree of reproducibility. The COV is reported here as the percentage of the mean value: values closer to 0% indicate lower variation and higher degree of reproducibility. Similarity is reported as a percentage, with 100% representing a perfect reproducibility.

3. Results

3.1. Literature search & bias assessment

The PubMed/MEDLINE and Embase search led to retrieval of 1348 unique articles (Fig. 1), which resulted in a final selection (Table 1) of 22 articles on animal studies (Argyridis et al., 2014; Chen et al., 2017; Deloire-Grassin et al., 2000; Duhamel et al., 2019; Fjær et al., 2015; Hakkarainen et al., 2016; Harkins et al., 2013; Janve et al., 2013; Jung et al., 2017; Khodanovich et al., 2017, 2019; Kozlowski et al., 2008; Lauri J. Lehto et al., 2017a; Lauri Juhani Lehto et al., 2017; Lodygensky et al., 2012; Merkler et al., 2005; Soustelle et al., 2019; Thiessen et al., 2013; Turati et al., 2015; Underhill et al., 2011; West et al., 2016; Zaaraoui et al., 2008) and 13 articles on human post-mortem studies (Bagnato et al., 2018a; Hametner et al., 2018; Laule et al., 2006, 2008; Mottershead et al., 2003; Reeves et al., 2016;

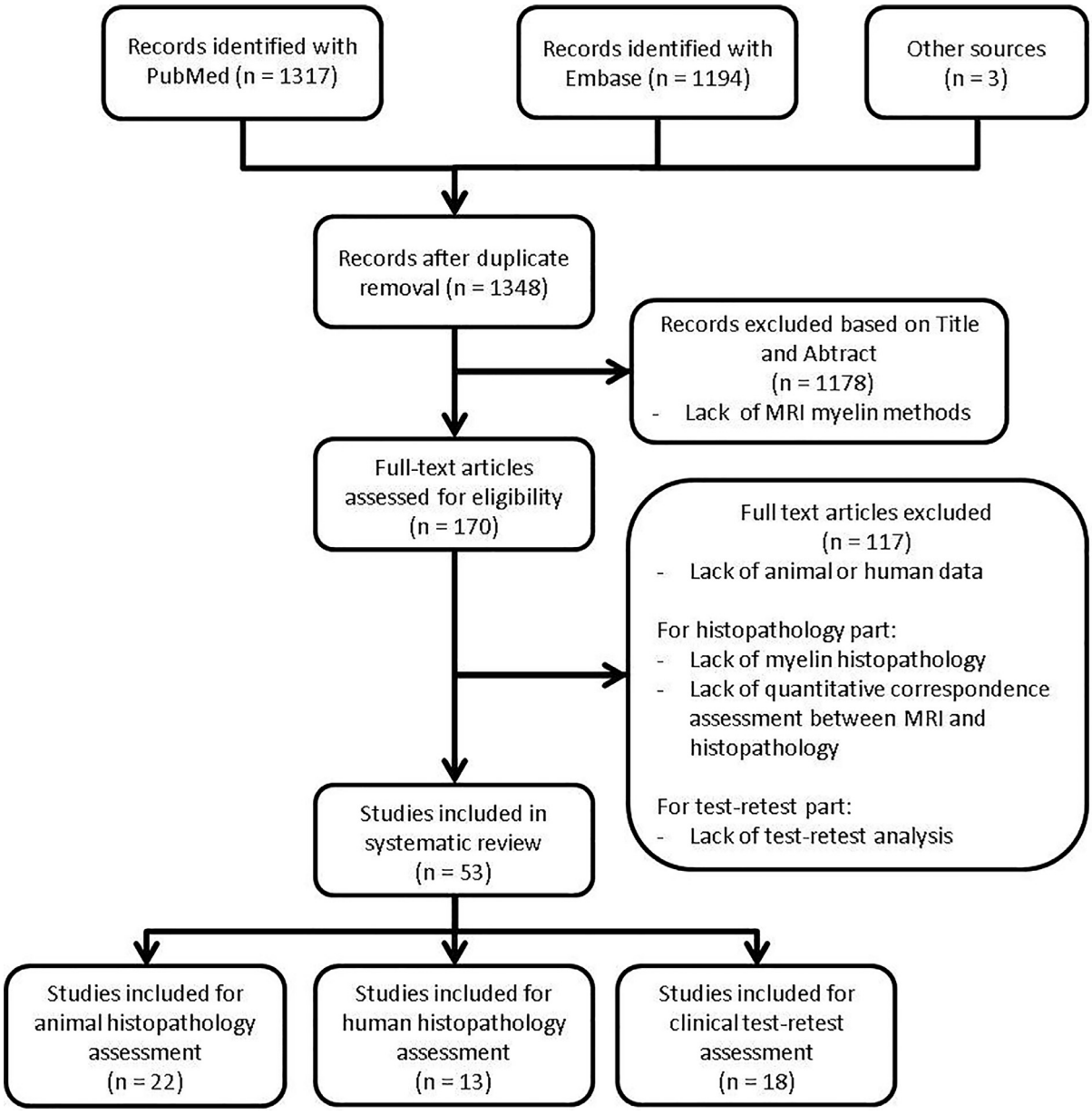

Fig. 1. Flow diagram of literature search.

Schmierer et al., 2004, 2007, 2008; Tardif et al., 2012; Van Der Voorn et al., 2011; Warntjes et al., 2017; Wiggermann et al., 2017) that validated MRI against histology quantitatively (Table 2-3). No animal studies were found that assessed the correspondence between the T1w/T2w ratio, R2*, qihMT, SyMRI, or mcDESPOT and myelin histology (Table 1), whereas no human studies were found that assessed the correlation between the T1w/T2w ratio, ihMTR, qihMT, UTE, mcDESPOT, or g-ratio and myelin histology quantitatively. In total, 18 studies (Arshad et al., 2017; Bagnato et al., 2018b, 2019; Drenthen et al., 2019; Duval et al., 2018; Ellerbrock and Mohammadi, 2018; Feng et al., 2018; Fujita et al., 2019; Lee et al., 2015; Levesque et al., 2010; Lévy et al., 2018; Ljungberg et al., 2017; Meyers et al., 2009; Nguyen et al., 2016; Prasloski et al., 2012; Shams et al., 2019; Wu et al., 2006; Zhang et al., 2019) examining reproducibility (all in humans) were retrieved (Table 4). The reproducibility of MWF measurements was evaluated in 8 studies (Arshad et al., 2017; Drenthen et al., 2019; Levesque et al., 2010; Ljungberg et al., 2017; Meyers et al., 2009; Nguyen et al., 2016; Prasloski et al., 2012; Wu et al., 2006), the repeatability of the T1w/T2w ratio in 3 studies (Arshad et al., 2017; Lee et al., 2015; Shams et al., 2019), qMT (Bagnato et al., 2019, 2018b) and g-ratio (Duval et al., 2018; Ellerbrock and Mohammadi, 2018) was assessed in 2 studies, whereas the test-retest analysis of T1 (Shams et al., 2019), MTR (Lévy et al., 2018), ihMTR (Zhang et al., 2019), qihMT (Zhang et al., 2019), SyMRI (Fujita et al., 2019), R2* (Feng et al., 2018), and QSM (Feng et al., 2018) was described in only a single study. No studies were found that conducted test-retest analysis for the other myelin MRI methods. All retrieved studies were classified with either a low or unclear bias risk (for an extensive analysis see Appendix).

3.2. *Methodology in animal studies*

The selected animal studies used either rats (Chen et al., 2017; Deloire-Grassin et al., 2000; Hakkarainen et al., 2016; Harkins et al., 2013; Janve et al., 2013; Kozlowski et al., 2008; Lauri J. Lehto et al., 2017; Lauri Juhani Lehto et al., 2017; Lodygensky et al., 2012;

Table 1
Summary of search results per validation part for each MRI myelin method.

	Preclinical		*Clinical*		*Test-retest*	
	# studies	# sample	# studies	# sample	# studies	# sample
T1	2	15	6	91	1	17
T2	3	30	4	34	-	-
T1w/T2w ratio	-	-	-	-	3	83
MWF	5	73	2	28	8	87
mcDESPOT	-	-	-	-	-	-
R2*	-	-	2	14	1	8
QSM	2	29	2	11	1	8
MTR	10	145	6	98	1	16
qMT	10	124	2	52	2	31
ihMTR	1	3	-	-	1	5
qihMT	-	-	-	-	1	5
SyMRI	-	-	1	12	1	10
UTE	1	15	-	-	-	-
g-ratio	1	12	-	-	2	19

* ihMT = inhomogenous magnetization transfer, mcDESPOT = multicomponent Driven Equilibrium Single Pulse Observation of T1 and T2, MTR = Magnetization Transfer Ratio, MWF = Myelin Water Fraction, qMT = quantitative Magnetization Tranfer, QSM = Quantitative Susceptibility Mapping, SyMRI = Synthetic MRI, UTE = ultrashort echo time

Table 2
Methods used to assess the correlation of MRI with myelin histology in animal studies.

Study	*Histological measurement*	*Ex vivo vs in vivo MRI*	*Post mortem interval*	*MRI method*	*Correlation method*
Deloire-Grassin, 2000	LM + toluidine blue	*In vivo*	1h	MTR	Spearman
Merkler, 2005	LFB	*In vivo*	Overnight	MTR	Pearson
Kozlowski, 2008	LFB	*Ex vivo*	Overnight	MWF	Pearson
Zaaraoui, 2008	anti-MBP Ab	*In vivo*	1h	MTR	Pearson
Underhill, 2011	LFB	*In vivo*	n.s.	qMT	Pearson
Lodygensky, 2012	black gold II	*In vivo*	1d	QSM	Spearman
Harkins, 2013	LM + toluidine blue	*In vivo*	2d	MWF, qMT	Not specified
Janve, 2013	LFB	*Ex vivo*	1d	MTR	Pearson
Thiessen, 2013	TEM	*In vivo*	>3d	T1,T2, MTR, qMT	Spearman
Argyridis, 2014	LFB	*Ex vivo*	Overnight	QSM	Not specified
Fjaer, 2015	anti-PLP Ab	*In vivo*	7d	MTR	Not specified
Turati, 2015	anti-MBP Ab	*In vivo*	Overnight	qMT	Spearman
	black gold II	*In vivo*	Overnight	qMT	Spearman
Hakkarainen, 2016	Gold chloride	*Ex vivo*	Overnight	T1, T2, MTR	Pearson
Lehto, 2017b	gold chloride	*Ex vivo*	4h	MTR	Pearson
West, 2016	TEM + toluidine blue	*Ex vivo*	1w	T2, MWF, MTR, qMT	Pearson
Chen, 2017	TEM	*Ex vivo*	Overnight	MWF	Not specified
Jung, 2017	TEM + toluidine blue	*Ex vivo*	1w	g-ratio	Not specified
Khodanivich, 2017	LFB	*In vivo*	Overnight	qMT	Pearson
Lehto, 2017a	gold chloride	*In vivo*	4h	MTR	Pearson
Duhamel, 2019	GFP	*In vivo*	2h	ihMTR	Pearson
Khodanovich, 2019	anti-MBP Ab	*In vivo*	1d	qMT	Linear regression
Soustelle, 2019	anti-MBP Ab	*Ex vivo*	2w	MWF, qMT, UTE	Spearman

anti-MBP Ab = anti-Myelin Basic Protein antibodies
anti-PLP Ab = anti-Proteolipid Protein antibodies
LFB = Luxol Fast Blue
LM = Light microscopy
MRI = magnetic resonance imaging
MTR = Magnetization Transfer Ratio
MWF = Myelin Water Fraction
n.s. = not specified
qMT = quantitative Magnetization Transfer
QSM = Quantitative Susceptibility Mapping
TEM = transmission electron microscopy

Underhill et al., 2011) or mice (Argyridis et al., 2014; Duhamel et al., 2019; Fjær et al., 2015; Jung et al., 2017; Khodanovich et al., 2019, 2017; Merkler et al., 2005; Soustelle et al., 2019; Thiessen et al., 2013; Turati et al., 2015; West et al., 2016; Zaaraoui et al., 2008) and these were either healthy animals or models for multiple sclerosis, glioma, traumatic brain injury, spinal cord injury, or intra-myelinic edema (Table 2 & A.1). The main difference in methodology was the use of *in-vivo* (Fig. 2A) or *ex-vivo* MRI measurements (Fig. 2B) and the histological technique used for myelin assessment. After *in-vivo* MRI, samples were harvested and fixated prior to histological assessment. With *ex-vivo* MRI, samples were first harvested and fixated, before MRI and histology. Overall, no significant differences were observed between *ex-vivo* and *in-vivo* MRI studies and their correlation with myelin histology (Fig. 3A Mann-Whitney U test, U=227.5, p=0.068). When each MRI method was individually assessed, there was also no difference between *ex-vivo* and *in-vivo* MRI observed.

Different histological techniques for myelin quantification were used: histochemistry, immunohistochemistry, or quantitative mi-

Table 3
Methods used to assess the correlation of MRI with myelin histology in human studies.

Study	*Histology measurement*	*Fixation method before MRI*	*Post-mortem interval*	*MRI method*	*Correlation method*
Mottershead, 2003	LFB	Not applicable	72h (SD 39.2h)	T1, T2, MTR	Spearman
Schmierer, 2004	LFB	Not applicable	35.9h (SD 12.4h)	T1, MTR	Pearson
Laule, 2006	LFB	10% formalin	>2m	MWF	Not specified
Schmierer, 2007	LFB	Not applicable	43h (SD 8h)	T1, MTR, qMT	Pearson
Laule, 2008	LFB	10% formalin	>2m	MWF	Not specified
Schmierer, 2008	LFB	Not applicable	51h (SD 28h)	T1, T2, MTR, qMT	Not specified
		10% formalin	8-133d (mean 64d, SD 42d)	T1, T2, MTR, qMT	Not specified
Van Der Voorn, 2011	LFB	Formalin	>5w	MTR	Pearson
Tardif, 2012	anti-MBP Ab	10% formalin	4y	T1, T2, MTR	Spearman
Reeves, 2016	anti-MBP Ab	Formalin	5-568d	T1, T2	Spearman
Warntjes, 2017	LFB	Not applicable	20h-3d	SyMRI	Spearman
Wiggermann, 2017	LFB	4% paraformaldehyde	unknown	QSM	Not specified
Bagnato, 2018a	LFB & anti-PLP Ab	4% paraformaldehyde	>1y	R2*	Pearson
Hametner, 2018	LFB	37% formalin	24d	QSM	Pearson

anti-MBP Ab = anti-Myelin Basic Protein antibodies
LFB = Luxol Fast Blue
MRI = magnetic resonance imaging
MTR = Magnetization Transfer Ratio
MWF = Myelin Water Fraction
qMT = quantitative Magnetization Transfer
QSM = Quantitative Susceptibility Mapping
SyMRI = Synthetic MRI

Table 4
Characteristics of the test–retest studies.

Study	*MRI method*	*TRT interval*	*Statistical correspondence analysis*
Wu, 2006	MWF	different days	COV
Meyers, 2009	MWF	2.5 h (1.5–3.75 h)	Pearson
Levesque, 2010	MWF	directly after each other	COV
Prasloski, 2012	MWF	2.5 h (1.5–3.75 h)	COV & unknown correlation (R^2 is mentioned)
Lee, 2015	T1w/T2w ratio	directly after each other	COV
Nguyen, 2016	MWF	After repositioning	COV & Pearson
Arshad, 2017	T1w/T2w ratio	5 min, with repositioning	ICC
Ellerbrock, 2018	g-ratio	1w (6-8d)	% similarity
Ljungberg, 2017	MWF	directly after each other	COV
Bagnato, 2018b	qMT	<1 month	COV
Duval, 2018	g-ratio	After repositioning	Pearson
Feng, 2018	QSM, R2*	3–38d	ICC & VR
Lévy, 2018	MTR	5d or 10 months	ICC
Bagnato, 2019	qMT	Directly after each other	Difference
Drenthen, 2019	MWF	After repositioning	ICC
Fujita, 2019	SyMRI	After repositioning	COV
Shams, 2019	T1, T1w/T2w ratio	After repositioning	Difference
Zhang, 2019	ihMTR, qihMT	3d & 45d	ICC

COV = Coefficient Of Variance
ICC = Intraclass Correlation Coefficient
ihMTR = inhomogeneous Magnetization Transfer Ratio
MRI = magnetic resonance imaging
MTR = Magnetization Transfer Ratio
MWF = Myelin Water Fraction
qihMT = quantitative inhomogeneous Magnetization Transfer
qMT = quantitative Magnetization Transfer
QSM = Quantitative Susceptibility Mapping
TRT = test-retest
VR = variance ratio

croscopy. Potential confounding effects of the histological methods for myelin assessment were investigated using Kruskal-Wallis analysis, but no significant differences between these histological methods were observed (H=3.330, p=0.189, data not shown).

3.3. Methodology in human studies

The correlation between *ex-vivo* myelin MRI and histology was assessed on post-mortem CNS samples from healthy subjects, or patients with epilepsy, Alzheimer's disease, MS, or X-linked adrenoleukodystrophy (Table 3 & A.2). The main differences in methodology were the use of either fresh samples or fixated samples (Fig. 2C & 2D) and the type of histological staining that was applied. The use of fixated or non-fixated samples (Fig. 3B) did not have a significant effect on the correlation between MRI and histology (Mann-Whitney U test, U=77, p=0.249). Either histochemistry or immunohistochemistry was used for histological assessment of myelin. No significant effect of the histological technique on the correlation with MRI was observed when assessing all MRI methods combined (U=28, p=0.148), or when MRI methods were individually assessed.

All reproducibility assessment studies were performed using *in vivo* MRI in healthy subjects (Table 4 & A.3). Different intervals between

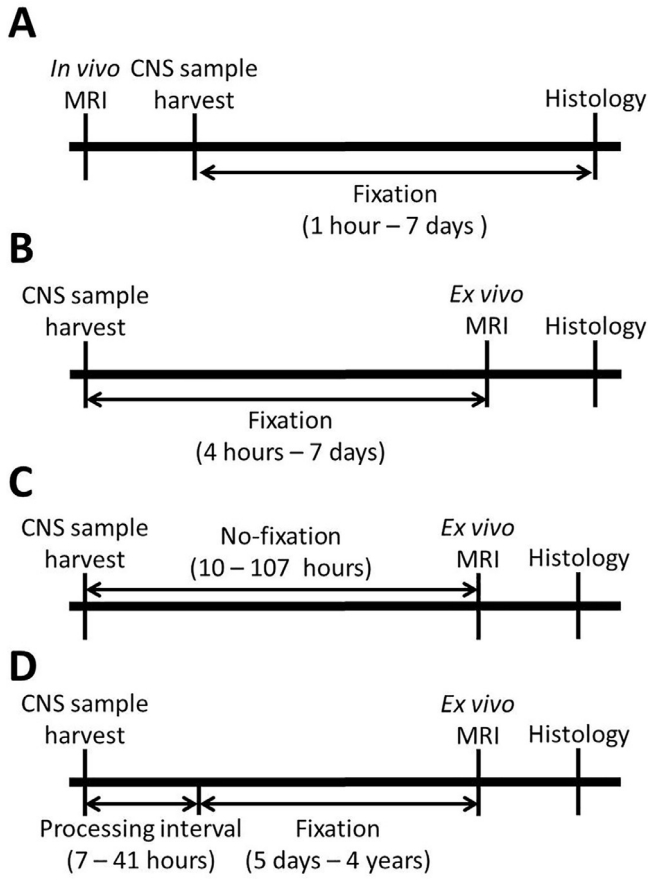

Fig. 2. Experimental methodology of myelin MRI validation studies. In animals, correlating MRI results with myelin histology, either (A) *in vivo* MRI (Deloire-Grassin et al., 2000; Duhamel et al., 2019; Fjær et al., 2015; Harkins et al., 2013; Khodanovich et al., 2019, 2017; Lauri J. Lehto et al., 2017; Lodygensky et al., 2012; Merkler et al., 2005; Thiessen et al., 2013; Turati et al., 2015; Underhill et al., 2011; Zaaraoui et al., 2008) or (B) *ex vivo* MRI (Argyridis et al., 2014; Chen et al., 2017; Hakkarainen et al., 2016; Janve et al., 2013; Jung et al., 2017; Kozlowski et al., 2008; Lauri Juhani Lehto et al., 2017; Soustelle et al., 2019; West et al., 2016) was used. After *in vivo* MRI, CNS samples were harvested for histological assessment. With *ex vivo* MRI, CNS samples were extracted before MRI and histology. The histological correspondence studies with human samples used for MR imaging either (C) fixated samples (Bagnato et al., 2018a; Hametner et al., 2018; Laule et al., 2008, 2006; Reeves et al., 2016; Schmierer et al., 2008; Tardif et al., 2012; Van Der Voorn et al., 2011; Wiggermann et al., 2017), or (D) fresh samples (Mottershead et al., 2003; Schmierer et al., 2008, 2007, 2004; Warntjes et al., 2017), then *ex-vivo* MRI was performed, followed by histological staining.

scan and rescan were used (range: immediate to 10 months). The three main methods applied were direct rescan after the first scan (Bagnato et al., 2019; Lee et al., 2015; Levesque et al., 2010; Ljungberg et al., 2017), direct rescan with repositioning after the first scan (Arshad et al., 2017; Drenthen et al., 2019; Duval et al., 2018; Fujita et al., 2019; Nguyen et al., 2016; Shams et al., 2019) or an interval of 2.5 h to 10 months between scan and rescan (Bagnato et al., 2018b; Ellerbrock and Mohammadi, 2018; Feng et al., 2018; Lévy et al., 2018; Meyers et al., 2009; Prasloski et al., 2012; Shams et al., 2019; Wu et al., 2006; Zhang et al., 2019). The direct scan-rescan evaluation was done for eliminating possible methodological confounding effects. The direct scan–rescan evaluation with repositioning was used to assess the sensitivity of the method regarding differences in orientation. The results were comparable to the scan-rescan protocol with intervals from 2.5 h to 10 months. On formal assessment, these differences in methodology did not show a significant influence on the test-retest analysis.

3.4. MRI correspondence with myelin histology in animals

The overall correspondence of all MRI methods combined with myelin histology is R^2=0.54 (SD=0.30, n=446). Forest plot analysis (Fig. 4A) of individual MRI methods shows that ihMTR has the highest correspondence with myelin histology (R^2=0.94, n=3, N=1), followed by QSM (R^2=0.85, n=29, N=2), g-ratio (R^2=0.69, n=12, N=1), qMT (R^2=0.60, n=124, N=10), MWF (R^2=0.55, n=73, N=5), T1 (R^2=0.55, n=15, N=2), UTE (R^2=0.51, n=15, N=1), MTR (R^2=0.42, n=145, N=10), and T2 (R^2=0.37, n=30, N=3). R^2 values per MRI method for individual studies are provided in Table 5.

3.5. MRI correspondence with myelin histology in humans

Overall, correspondence of the combined *ex-vivo* human myelin MRI methods with histology is R^2=0.54 (SD=0.18, n=340). The studies correlating MRI with histology in humans are summarized in Fig. 4B. Forest plot analysis of individual MRI methods showed that the highest MRI-histological correspondence was found for MWF (R^2=0.68, n=28, N=2), followed by MTR (R^2=0.65, n=98, N=6), qMT (R^2=0.60, n=52, N=2), SyMRI (R^2=0.55, n=12, N=1), T1 (R^2=0.48, n=91, N=6), T2 (R^2=0.45, n=34, N=4), R2* (R^2=0.18, n=14, N=2), and QSM (R^2=0.07, n=11, N=2). Reported results per individual study with human data are displayed in Table 6.

3.6. Reproducibility assessment

Various outcome measures were used for analysis of the reproducibility (Table A.4). High test-retest reproducibility was reported for MWF with COV 1.3–27%, R^2 0.90–0.99, and ICC 0.88–0.93. The variability in COV values is due to differences in test-retest outcomes between brain regions, with worst reproducibility in areas with poorest B1 field homogeneity. For the T1w/T2w ratio, also a high reproducibility between scans is reported, with 3.4% COV, 0.91 ICC, and a difference of 1.0–3.9%. The test-retest analysis for g-ratio displayed a R^2 of 0.19 and 86% similarity. Furthermore, a COV of 0.6-3.5% for SyMRI, an ICC of 0.92 for R2*, a difference of 0.6–2.5% for T1, an ICC of 0.87–0.91 for QSM, an ICC of 0.05–0.51 for MTR, a COV of 1.4–11.4% and a difference of 0.0–0.6% for qMT, an ICC of 0.81 for ihMTR, and an ICC of 0.86 for qihMT were observed. In general, test–retest reproducibility was adequate except for MTR.

4. Discussion

Accurate and reliable measurement of myelin density would greatly facilitate the evaluation of treatment strategies in MS that are focused on myelin repair. This review aimed to investigate the performance of currently available MRI methods for myelin quantification with respect to the correspondence with histology, and reproducibility. Our findings indicate that overall the MRI methods show a fairly good correlation with histology and a good test–retest variability. However, the available data from animal models, *ex-vivo* studies on human brains, and *in-vivo* repeatability studies is still limited for most MRI methods, thus precluding a definite conclusion on the most optimal MRI method for myelin quantification. Besides, differences in methodology between studies also hamper a thorough comparison, underlining the need for standardization of methods.

Differences in sample preparation, especially the use of fixation, was suggested to negatively influence MRI correspondence with myelin histology (Schmierer et al., 2008). Our analysis found no significant effect, but a trend towards an effect of sample preparation on the correlation between MRI and histology in animal studies (*in-vivo* vs. *ex-vivo* MRI) was observed. This indication was not found in human studies (fresh vs. fixated samples). It has been suggested that the fixation process interacts with relevant macromolecules, thereby altering their physical

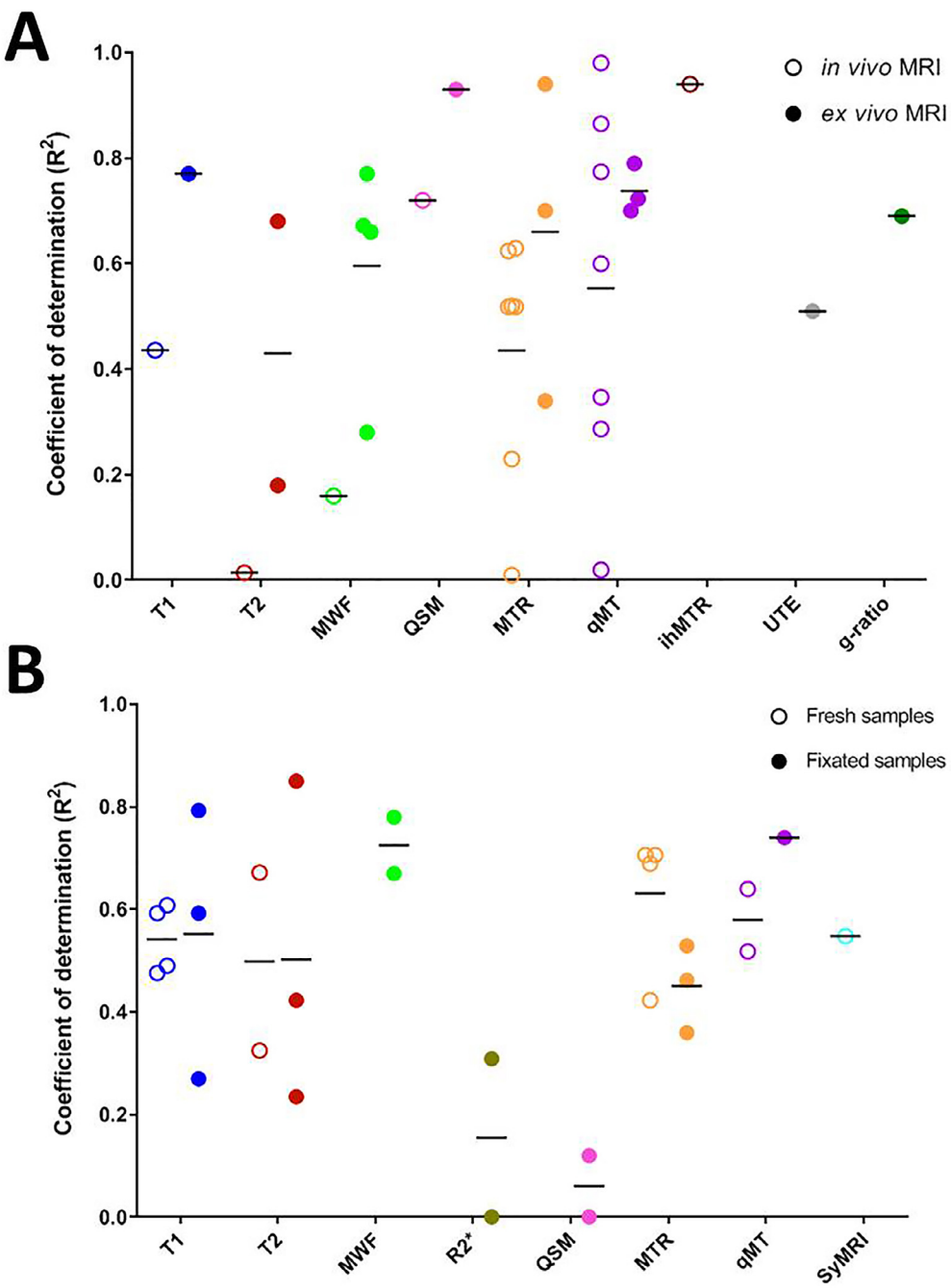

Fig. 3. Results of individual studies assessing the histological correspondence with various MRI methods. For animal studies (A), open symbols depict *in vivo* MRI studies, closed symbols *ex vivo* MRI studies, and the lines depict unweighted mean values. For studies using human samples (B), open symbols depict the use of fresh CNS samples, closed symbols represent fixated CNS samples, and the lines depict unweighted mean values. MTR = magnetization transfer ratio, MWF = myelin water fraction, qMT = quantitative Magnetization Transfer, QSM = quantitative susceptibility mapping, SyMRI = Synthetic MRI.

characteristics and thus magnetization transfer between these macromolecules and the free water pool (Schmierer et al., 2010). However, the fact that similar results were obtained when fresh and fixated human samples (both *ex-vivo* MRI) were used, indicates that the effect of sample preparation in animal studies is probably not caused by the fixation process per se, but is likely also due to a difference in acquisition of the imaging signal between *in-vivo* and *ex-vivo* samples, such as distortion of magnetic field homogeneity.

A high variability in the performance of the same MRI technique between studies was observed. The intrinsic clinical nature of MRI requires optimization of the signal to noise ratio (SNR) and the contrast to noise ratio (CNR) by adjusting the MRI parameters to obtain the best images with the most diagnostic information per individual, which inherently also affects reproducibility. Changes in e.g. repetition time (TR) or echo time (TE) have huge impact on voxel intensity. Even when these parameters remain constant, changes in patient orientation within the field-of-view (FOV) cause differences in tissue composure, and hence also leading to differences in voxel intensities. These aspects make it difficult to perform reproducible and quantitative analysis. As illustrated in the Appendix (Table A.5-17), this leads to a high variety among the MR parameters within the same methodology. These results suggest that the high variation in efficacy for T1, T2, MTR, and qMT (Fig. 3) is likely due to the variety of settings in TE, TR, flip angle, off-set frequencies, and sequences used to generate these images (Table A.5-6,11-12). In contrast, the low variation in results for MWF in human (as compared to animal studies) may be due to the fact that these studies have been performed in a single centre, thus reducing the number of variables between studies. Standardized protocols with one consistent FOV large enough for every brain, using consequently the same TR, TE, inversion time (TI), flip angles, matrix sizes, etc. would enhance MRI reproducibility and would aid in quantitative MRI analysis.

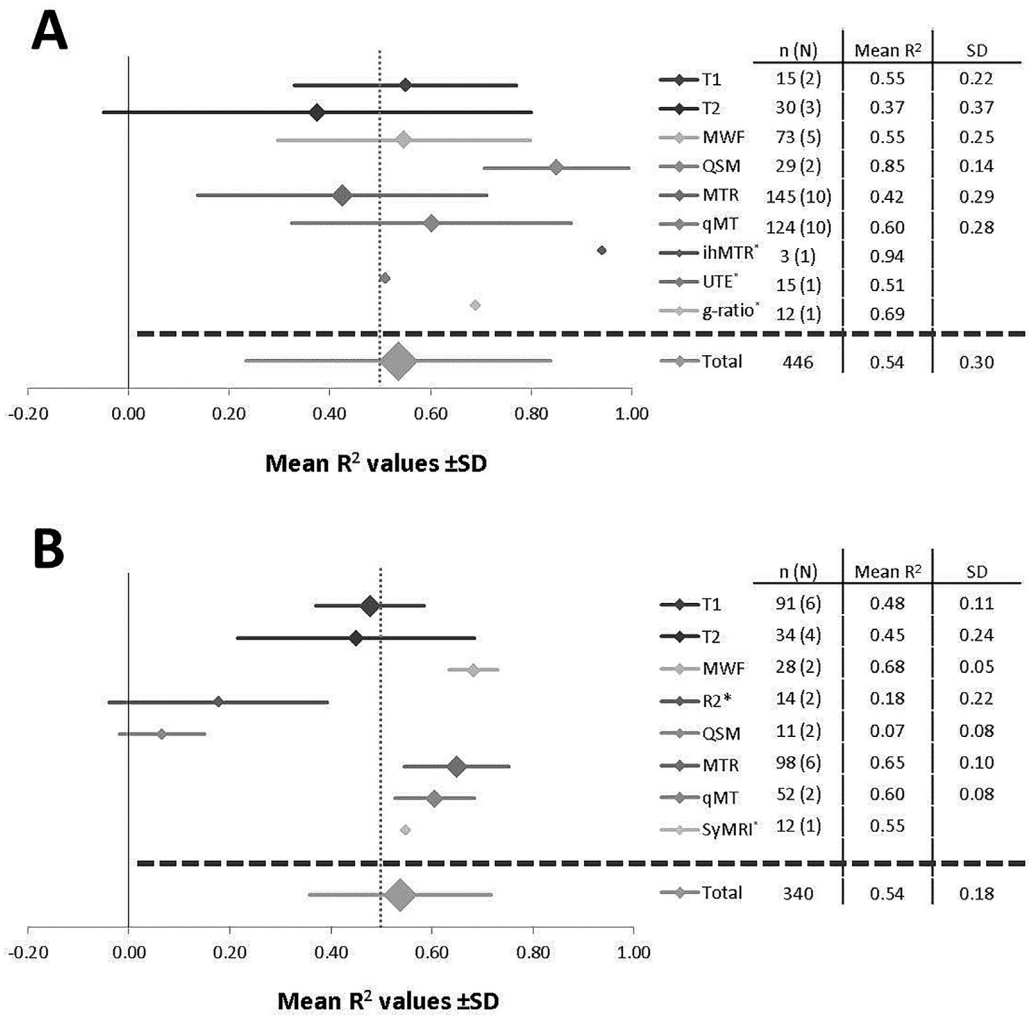

Fig. 4. Forest plot analysis of correspondence (R^2) between myelin MRI and histology. The animal studies are depicted in (A), the human studies in (B). MTR = magnetization transfer ratio, MWF = myelin water fraction, n = sample size, N = number of studies, qMT = quantitative Magnetization Transfer, QSM = quantitative susceptibility mapping, SD = standard deviation, SyMRI = Synthetic MRI. · no SD, since only one study was available

The correspondence between the different MRI methods and histology ranges from R^2 0.37 (from 3 studies assessing T2) to 0.94 (of the one study assessing ihMTR) in animal studies and from 0.07 to 0.68 in human studies. In human studies, MWF, MTR, and qMT gave the highest correspondence with myelin histology with R^2 values of 0.68, 0.65, and 0.60, respectively. These results indicate that the ground work for myelin imaging with MRI is present, and further improvement and optimization might improve the accuracy to measure myelin density. When the difference between *ex-vivo* and *in-vivo* animal studies is translated to humans, it can be expected that *in-vivo* assessment of myelin in the human brain will show a somewhat lower correlation with myelin content than the current *ex-vivo* measurements. Recent data indicate that differences in iron content seem to have a major impact on the MWF signal (Birkl et al., 2019), but further studies are needed to improve the myelin specificity of MWF, for example by introducing correction for iron content. Iron is a dominant contributor to R2* and QSM measurements, in particular in grey matter. In white matter iron concentrations are thought to be low and thus have less impact on the MWF, but R2* and QSM measurements seem to be highly susceptible for white matter microstructure and fibre orientation, which hampers their use for myelin imaging and supports the lack of associations with myelin histological assessment in humans (Gil et al., 2016; Oh et al., 2013). Recently, the T1w/T2w ratio and mcDESPOT have already been used as myelin MRI measurements in human studies correlating their results to clinical characteristics, despite the fact that no animal or human studies quantitatively investigating the correspondence between MRI estimates and myelin histology for these techniques have been reported yet (Ganzetti et al., 2014; Kolind et al., 2015). However, mcDESPOT has been demonstrated to be an inaccurate and imprecise measurement, when magnetization exchange is present, even if intercompartment exchange is removed from the underlying microstructural model (West et al., 2019). Although several examples have been reported that suggest precise mcDESPOT MWF estimates can be obtained, this apparent MWF contrast is likely due to bias introduced by the Stochiastic Region Contraction method commonly used to fit the mcDESPOT model. As a result of this bias, mcDESPOT-derived parameter estimates can only be compared between studies if similar acquisition and analysis protocols are used. The T1w/T2w ratio has a poor correlation with MWF, indicating that the T1w/T2w ratio does not measure the myelin water fraction (Uddin et al., 2018). Very recently, a technique called Ultrashort EchoTime or UTE has also been applied to myelin imaging. This method would have the potential to directly image macromolecular-bound hydrogen in myelin (Du et al., 2014). Our analysis found only 1 article assessing the performance of UTE, showing a moderate correspondence with myelin histology in animals. Possibly, different strategies e.g. the use of a UTE devoid of diffusion weighing might potentially enhance UTE's efficacy for myelin imaging.

Table 5
R^2 values for the correlation of different MRI methods with myelin histology data observed in animal studies.

Study	ROI origin	T1	T2	MWF	QSM	MTR	qMT	ihMTR	UTE	g-ratio	Sample size
Deloire-Grassin, 2000	WM					0.63					5
Merkler, 2005	WM					0.23					35
Kozlowski, 2008	WM			0.77							16
Zaaraoui, 2008	WM					0.62					16
Underhill, 2011	GM & WM						0.98				9
Lodygensky, 2012	WM				0.72						11
Harkins, 2013	WM			0.16			0.02				9
Janve, 2013	WM						0.72				9
Thiessen, 2013	WM	0.44	0.53			0.52	0.86				10
Argyridis, 2014	WM				0.93						18
Fjaer, 2015	GM & WM					0.01					24
Turati, 2015	WM						0.35				15
	WM						0.29				15
Hakkarainen, 2016	GM & WM	0.77	0.18			0.34					5
Lehto, 2017b	GM					0.94					11
West, 2016	GM & WM		0.68	0.66		0.70	0.70				15
Chen, 2017	WM			0.67							18
Jung, 2017	WM									0.69	12
Khodanivich, 2017	GM & WM						0.77				14
Lehto, 2017a	WM					0.52					21
Duhamel, 2019	GM & WM					0.52		0.94			3
Khodanovich, 2019	GM & WM						0.60				13
Soustelle, 2019	GM & WM			0.28			0.60		0.51		15

GM = Grey matter
ihMTR = inhomogeneous Magnetization Transfer Ratio
MTR = Magnetization Transfer Ratio
MWF = Myelin Water Fraction
qMT = quantitative Magnetization Transfer
QSM = Quantitative Susceptibility Mapping
UTE = Ultrashort Echo Time
WM = White matter

Table 6
R^2 values for the correlation of different MRI methods with myelin histology data observed in studies on human material.

Study	ROI origin	T1	T2	MWF	R2*	QSM	MTR	qMT	SyMRI	Sample size
Mottershead, 2003	WM	0.61	0.33				0.42			4
Schmierer, 2004	WM	0.49					0.71			20
Laule, 2006	GM & WM			0.67						25
Schmierer, 2007	WM	0.48					0.71	0.64		37
Laule, 2008	GM & WM			0.78						3
Schmierer, 2008 unfix	WM	0.59	0.67				0.69	0.52		15
Schmierer, 2008 *fix*	WM	0.79	0.85				0.46	0.74		
Van der Voorn, 2011	WM						0.53			20
Tardif, 2012	GM & WM	0.59	0.42				0.36			2
Reeves, 2016	GM & WM	0.27	0.24							13
Warntjes, 2017	GM & WM								0.55	12
Wiggermann, 2017	WM					0.001				5
Bagnato, 2018a	GM & WM				0.31					8
Hametner, 2018	GM & WM				0.001	0.12				6

GM = Grey matter
MTR = Magnetization Transfer Ratio
MWF = Myelin Water Fraction
qMT = quantitative Magnetizaiton Transfer
QSM = Quantitative Susceptibility Mapping
SyMRI = Synthetic MRI
WM = White matter
There are no articles correlating myelin histology with T1w/T2w ratio or g-ratio myelin estimates.

Another explanation might be that the variability in the results between individual studies could be due to differences in the histological methods used. Because electron microscopy allows direct measurement of myelin sheaths it is considered the most reliable method. However, electron microscopy is elaborate and only gives information about a small part of the tissue. Immunohistochemistry methods that target either myelin basic protein (MBP) or proteolipid protein (PLP) are then considered most accurate, followed by histochemistry methods, like luxol fast blue (LFB), that target lipophilic structures. However, a head-to-head comparison of all of these histological methods has not been published, which would be necessary for thoroughly assessing the efficacy of the various myelin histological methods for quantifying myelin. Nonetheless, our analysis did not show a significant confounding effect of the histological methods used in the animal studies or in the human studies, although one of the underlying animal studies actually observed a very strong effect between the use of LFB and anti-MBP antibodies (Kozlowski et al., 2008).

In our study, we combined all available animal studies for analysis of the quantitative correspondence between MRI and myelin histology. According to our forest plot analysis of animal studies, ihMTR and QSM

have by far the highest correspondence with myelin histology, followed by g-ratio, qMT, MWF, and T1. Others (Thiessen et al., 2013; West et al., 2016) performed a head-to-head comparison, showing that qMT performs better than T1 and T2. In contrast, another study indicated that T2, MWF, MTR and qMT have a similar performance (West et al., 2016) and a third study demonstrated that T2 performs better than both T1 and MTR (Merkler et al., 2005). This discrepancy between studies suggests a strong effect of experimental design and local factors on the outcome of such comparisons. This observation is corroborated by the results of human studies, which also display a high variety among individual studies. Our forest plot analysis for human studies shows that MWF performs slightly better than the other MRI methods, although not enough data are available to support a firm statement. Also, no head-to-head comparisons of MWF with other myelin MRI techniques in humans have been described so far. Interestingly, the high correspondence of QSM with myelin histology observed in animals, could not be confirmed in the first studies with human samples. The failure of QSM to display changes in myelin in human studies, might be due to the differences in susceptibility gradients between *in-vivo* and *ex-vivo* tissue, and the current QSM post processing algorithms employed (Wiggermann et al., 2017). This suggests that QSM has potential, but further optimization and improvement of this method in humans is needed. Head-to-head comparisons between different MRI methods for myelin imaging in the human brain also give conflicting results (Mottershead et al., 2003; Schmierer et al., 2007, 2004; Tardif et al., 2012). Two studies on fresh CNS samples show that T1 performs better than T2 and MTR (Mottershead et al., 2003; Tardif et al., 2012), whereas another study on fresh CNS samples suggests that MTR and qMT perform better than T1 (Schmierer et al., 2007). More recently, the same authors found that T1, T2, MTR and qMT have a similar performance in fresh samples (Schmierer et al., 2008), whereas MTR performed worse than the other methods in fixated samples (Schmierer et al., 2008). In the study of Alonso-Ortiz and colleagues (Alonso-Ortiz et al., 2018) a higher correspondence between different MWF estimates was observed when regions in both WM and GM were investigated, instead of only WM regions. In our study, correlations between myelin histology and MRI measures in both WM and GM were not better than the same correlations in only WM or only GM regions (Tables 5-6 and A.4). Currently, no study with either animal or human samples provided a direct comparison of all myelin MRI techniques. Comparing all myelin MRI methods with myelin histology within the same brain sample set would facilitate the selection of the most reliable myelin MRI method. Such a brain sample set should include various diseases and disease stages. At the same time, combinations of several methods could be assessed in order to evaluate if such a multiparametric imaging approach could yield a higher overall accuracy. According to the results of Mangeat and colleagues, such a multiparametric approach results in more accurate myelin estimations and could also easily be implemented for clinical use (Mangeat et al., 2015). Application in clinical practice should be feasible as acquisition times range from 4 (MWF) to 7 minutes (mcDESPOT) (Cercignani et al., 2017; Hervé et al., 2011; Nguyen et al., 2016; Zhang et al., 2015).

The reproducibility of the evaluated MRI methods is generally good. However, data on reproducibility are scarce and only for MWF sufficient studies to assess reproducibility are available. The low reproducibility of MTR could be due to motion and susceptibility artefacts and the low signal-to-noise ratio achieved, as suggested by others (Lévy et al., 2018). They state these effects are specifically relevant in spinal cord imaging, however, other studies assessing the reproducibility of myelin MRI in spinal cord imaging did not observe this (Duval et al., 2018; Ljungberg et al., 2017; Wu et al., 2006). The low reproducibility of MTR in the study of Levy and colleagues might therefore also be caused by other factors, such as the variable interval between the scans (5 days or 10 months) or to the used off-set frequency of the RF pulse of 1.2 kHz, which does not result in optimal saturation (7–10 kHz) (Ulmer et al., 1996). In addition, when comparing studies that correlated myelin MRI with histology in the brain and studies that evaluated myelin imaging in the spinal cord, no differences (data not shown) in accuracy were found, further supporting the assumption that the low reproducibility is most likely not due to spinal cord imaging. More studies are needed to determine the test-retest variability of the other MRI methods for myelin imaging. Noteworthy are the discrepant test-retest results for g-ratio: one study reported high reproducibility (Ellerbrock and Mohammadi, 2018), whereas another study found a low reproducibility (Duval et al., 2018). This might be due to differences in the applied diffusion MRI sequence. The landscape of sequences and biophysical models used in MRI is vast and inhomogeneous, especially for diffusion MRI. Regarding diffusion MRI, the same Pulsed Gradient Spin Echo (PGSE) sequence with different parameters can probe for hugely different physical and physiological parameters. The observation that for some myelin MRI methods (e.g. T1w/T2w ratio, qihMT) accuracy assessment through comparison with histology has not been performed yet, questions the worth of the reproducibility assessment for these imaging techniques.

Since no other myelin imaging techniques are currently routinely used in humans, we did not compare the MRI performance to other imaging techniques. Especially molecular imaging techniques like Positron Emission Tomography (PET) are by nature particularly suitable for quantitative analysis of tissue constituents. Preclinical PET studies with myelin binding ligands showed promising results (Auvity et al., 2020; de Paula Faria et al., 2014; Wu et al., 2010). Recently, also amyloid PET tracers have been successfully used for assessing myelin integrity in humans (Zeydan et al., 2018). Combining the spatial resolution of MRI with the quantitative power of PET may further improve reliable quantification of myelin *in-vivo*.

In conclusion, MRI-based myelin imaging methods overall show a fairly good correlation with histology and a good reproducibility. However, the currently available data is insufficient and the variability in performance between studies is too large to determine which MRI method reflects myelin content best. This indicates that all methodologies should be continued to pursue and motivates to perform more head-to-head comparisons across MRI methods and histology. Nonetheless, the highest correspondence between myelin MRI and myelin histology assessed by at least two independent studies was observed for QSM (R^2=0.85) in animals, whereas MWF correlated best (R^2=0.68) in humans. Optimization of the intrinsic properties of the MRI techniques to overcome methodological constraints and a thorough assessment of the quantitative nature of the myelin histological methods, might improve the accuracy of myelin MRI methods for myelin imaging. This analysis also underlines the need for further standardisation of protocols to facilitate the comparison of the results from different studies.

Data and code availability statement

Since this study is a systematic review, all data regarding this study were publicly available. This study was conducted in accordance with the PRISMA-DTA statement, using the databases of PubMed/MEDLINE and Embase. PubMed/MEDLINE and Embase were searched for studies on myelin MRI published until December 2019, using the search strings shown in the Appendix, without language restrictions.

Search string for PubMed/MEDLINE search:

- ("Myelin Sheath"[Mesh] OR "myelin sheath"[tiab] OR myelin[tiab] OR "myelin sheaths"[tiab]) AND (((quantification[tiab] OR quantitative[tiab]) AND ((“T1 T2 ratio”[tiab] OR “T1-T2 ratio”[tiab] OR “T1-T2-ratio”[tiab] OR “T1 T2”[tiab] OR T1[tiab]) OR (“Magnetic Resonance Imaging”[MeSH] OR MRI[tiab] OR “magnetic resonance imaging”[tiab] OR “MR imaging”[tiab] OR “MRI scan”[tiab] OR “MRI scans”[tiab]))) OR ("Proton Spin Tomography"[tiab] OR "Spin Echo Imaging"[tiab] OR "spin echo"[tiab] OR "spin-echo"[tiab] OR GRASE[tiab]) OR (“myelin water fraction”[tiab] OR “myelin water imaging”[tiab] OR “myelin volume fraction”[tiab] OR “multiexponential T2”[tiab] OR MWF[tiab] OR MVF[tiab] OR MWI[tiab] OR MET2[tiab] OR “myelin volume”[tiab] OR “myelin water”[tiab])

OR (QSM[tiab] OR “quantitative susceptibility mapping”[tiab] OR “quantitative susceptibility map”[tiab]) OR (mcDESPOT[tiab] OR “multicomponent driven”[tiab]) OR (g-ratio[tiab]) OR (“magnetic transfer”[tiab] OR “magnetization transfer”[tiab] OR “quantitative magnetic transfer”[tiab] OR “magnetic transfer ratio”[tiab] OR “magnetization transfer ratio”[tiab] OR “quantitative magnetization transfer”[tiab] OR MT[tiab] OR MTR[tiab] OR QMT[tiab]))

Search string for Embase:

- (‘Myelin Sheath’/exp OR myelin:ab,ti) AND (((quantification:ab,ti OR quantitative:ab,ti) AND ((‘T1 T2 ratio’:ab,ti OR ‘T1-T2 ratio’:ab,ti OR ‘T1-T2-ratio’:ab,ti OR ‘T1 T2’:ab,ti OR T1:ab,ti) OR (‘Magnetic Resonance Imaging’/exp OR MRI:ab,ti OR ‘magnetic resonance imaging’:ab,ti OR ‘MR imaging’:ab,ti OR ‘MRI scan*’:ab,ti OR ‘MRI scans’:ab,ti))) OR (‘Proton Spin Tomography’:ab,ti OR ‘Spin Echo Imaging’:ab,ti OR ‘spin echo’:ab,ti OR GRASE:ab,ti) OR (‘myelin water fraction’:ab,ti OR ‘myelin water imaging’:ab,ti OR ‘myelin volume fraction’:ab,ti OR ‘multiexponential T2’:ab,ti OR MWF:ab,ti OR MVF:ab,ti OR MWI:ab,ti OR MET2:ab,ti OR ‘myelin volume’:ab,ti OR ‘myelin water’:ab,ti) OR (QSM:ab,ti OR ‘quantitative susceptibility mapping’:ab,ti OR ‘quantitative susceptibility map’:ab,ti) OR (mcDESPOT:ab,ti OR ‘multicomponent driven’:ab,ti) OR (g-ratio:ab,ti OR ‘g ratio’:ab,ti) OR (‘magnetic transfer’:ab,ti OR ‘magn* transfer’:ab,ti OR ‘magnetization transfer’:ab,ti OR ‘quantitative magnetic transfer’:ab,ti OR ‘magnetic transfer ratio’:ab,ti OR ‘magnetization transfer ratio’:ab,ti OR ‘quantitative magnetization transfer’:ab,ti OR MT:ab,ti OR MTR:ab,ti OR QMT:ab,ti)) NOT ‘conference abstract’/it

Contributors

C.W.J.W., J.F.M., and E.F.J.V. designed the study, C.W.J.W. and E.F.J.V. did the search, data extraction, and publication bias assessment, C.W.J.W. and D.V.G. performed the statistical analysis. All authors contributed to the interpretation of the data, writing, and reviewing of the final report.

Declaration of Competing Interest

The authors declare no competing interests.

Acknowledgments

This study was supported by Nederlandse organisatie voor gezondheidsonderzoek en zorginnovatie (ZonMW) and Stichting MS research, grant number PTO-95105010.

Supplementary materials

Supplementary material associated with this article can be found, in the online version, at doi:10.1016/j.neuroimage.2020.117561.

References

Alizadeh, A., Dyck, S.M., Karimi-Abdolrezaee, S., 2015. Myelin damage and repair in pathologic CNS: challenges and prospects. Front. Mol. Neurosci. 8. https://doi.org/10.3389/fnmol.2015.00035.

Alonso-Ortiz, E., Levesque, I.R., Pike, G.B., 2018. Multi-gradient-echo myelin water fraction imaging: comparison to the multi-echo-spin-echo technique. Magn. Reson. Med.. https://doi.org/10.1002/mrm.26809.

Argyridis, I., Li, W., Johnson, G.A., Liu, C., 2014. Quantitative magnetic susceptibility of the developing mouse brain reveals microstructural changes in the white matter. Neuroimage. https://doi.org/10.1016/j.neuroimage.2013.11.026.

Arshad, M., Stanley, J.A., Raz, N., 2017. Test–retest reliability and concurrent validity of in vivo myelin content indices: myelin water fraction and calibrated T1w/T2w image ratio. Hum. Brain Mapp. 38, 1780–1790. https://doi.org/10.1002/hbm.23481.

Auvity, S., Tonietto, M., Caillé, F., Bodini, B., Bottlaender, M., Tournier, N., Kuhnast, B., Stankoff, B., 2020. Repurposing radiotracers for myelin imaging: a study comparing 18F-florbetaben, 18F-florbetapir, 18F-flutemetamol,11C-MeDAS, and 11C-PiB. Eur. J. Nucl. Med. Mol. Imaging. https://doi.org/10.1007/s00259-019-04516-z.

Bagnato, F., Franco, G., Ye, F., Fan, R., Commiskey, P., Smith, S.A., Xu, J., Dortch, R., 2019. Selective inversion recovery quantitative magnetization transfer imaging: toward a 3 T clinical application in multiple sclerosis. Mult. Scler. J.. https://doi.org/10.1177/1352458519833018.

Bagnato, F., Hametner, S., Boyd, E., Endmayr, V., Shi, Y., Ikonomidou, V., Chen, G., Pawate, S., Lassmann, H., Smith, S., Brian Welch, E., 2018a. Untangling the R2* contrast in multiple sclerosis: a combined MRI-histology study at 7.0 Tesla. PLoS One. https://doi.org/10.1371/journal.pone.0193839.

Bagnato, F., Hametner, S., Franco, G., Pawate, S., Sriram, S., Lassmann, H., Gore, J., Smith, S.E., Dortch, R., 2018b. Selective inversion recovery quantitative magnetization transfer brain MRI at 7T: clinical and postmortem validation in multiple sclerosis. J. Neuroimaging. https://doi.org/10.1111/jon.12511.

Birkl, C., Birkl-Toeglhofer, A.M., Endmayr, V., Hoftberger, R., Kasprian, G., Krebs, C., Haybaeck, J., Rauscher, A., 2019. The influence of brain iron on myelin water imaging. Neuroimage. https://doi.org/10.1016/j.neuroimage.2019.05.042.

Brück, W., Bitsch, A., Kolenda, H., Brück, Y., Stiefel, M., Lassmann, H., 1997. Inflammatory central nervous system demyelination: correlation of magnetic resonance imaging findings with lesion pathology. Ann. Neurol. 42, 783–793. https://doi.org/10.1002/ana.410420515.

Cercignani, M., Giulietti, G., Dowell, N.G., Gabel, M., Broad, R., Leigh, P.N., Harrison, N.A., Bozzali, M., 2017. Characterizing axonal myelination within the healthy population: a tract-by-tract mapping of effects of age and gender on the fiber g-ratio. Neurobiol. Aging 49, 109–118. https://doi.org/10.1016/j.neurobiolaging.2016.09.016.

Chen, H.S.-M., Holmes, N., Liu, J., Tetzlaff, W., Kozlowski, P., 2017. Validating myelin water imaging with transmission electron microscopy in a rat spinal cord injury model. Neuroimage 153, 122–130. https://doi.org/10.1016/j.neuroimage.2017.03.065.

de Paula Faria, D., De Vries, E.F.J., Sijbesma, J.W.A., Dierckx, R.A.J.O., Buchpiguel, C.A., Copray, S., 2014. PET imaging of demyelination and remyelination in the cuprizone mouse model for multiple sclerosis: a comparison between [11C]CIC and [11C]MeDAS. Neuroimage 87, 395–402. https://doi.org/10.1016/j.neuroimage.2013.10.057.

Deloire-Grassin, M.S.A., Brochet, B., Quesson, B., Delalande, C., Dousset, V., Canioni, P., Petry, K.G., 2000. In vivo evaluation of remyelination in rat brain by magnetization transfer imaging. J. Neurol. Sci. 178, 10–16. https://doi.org/10.1016/S0022-510X(00)00331-2.

Drenthen, G.S., Backes, W.H., Aldenkamp, A.P., Jansen, J.F.A., 2019. Applicability and reproducibility of 2D multi-slice GRASE myelin water fraction with varying acquisition acceleration. Neuroimage. https://doi.org/10.1016/j.neuroimage.2019.04.011.

Du, J., Ma, G., Li, S., Carl, M., Szeverenyi, N.M., VandenBerg, S., Corey-Bloom, J., Bydder, G.M., 2014. Ultrashort echo time (UTE) magnetic resonance imaging of the short T2 components in white matter of the brain using a clinical 3T scanner. Neuroimage. https://doi.org/10.1016/j.neuroimage.2013.10.053.

Duhamel, G., Prevost, V.H., Cayre, M., Hertanu, A., Mchinda, S., Carvalho, V.N., Varma, G., Durbec, P., Alsop, D.C., Girard, O.M., 2019. Validating the sensitivity of inhomogeneous magnetization transfer (ihMT) MRI to myelin with fluorescence microscopy. Neuroimage. https://doi.org/10.1016/j.neuroimage.2019.05.061.

Duval, T., Smith, V., Stikov, N., Klawiter, E.C., Cohen-Adad, J., 2018. Scan–rescan of axcaliber, macromolecular tissue volume, and g-ratio in the spinal cord. Magn. Reson. Med.. https://doi.org/10.1002/mrm.26945.

Ellerbrock, I., Mohammadi, S., 2018. Four in vivo g-ratio-weighted imaging methods: comparability and repeatability at the group level. Hum. Brain Mapp. 39, 24–41. https://doi.org/10.1002/hbm.23858.

Feng, X., Deistung, A., Reichenbach, J.R., 2018. Quantitative susceptibility mapping (QSM) and R2* in the human brain at 3 T: evaluation of intra-scanner repeatability. Z. Med. Phys.. https://doi.org/10.1016/j.zemedi.2017.05.003.

Fjær, S., Bø, L., Myhr, K.M., Torkildsen, O., Wergeland, S., 2015. Magnetization transfer ratio does not correlate to myelin content in the brain in the MOG-EAE mouse model. Neurochem. Int. 83–84, 28–40. https://doi.org/10.1016/j.neuint.2015.02.006.

Fujita, S., Hagiwara, A., Hori, M., Warntjes, M., Kamagata, K., Fukunaga, I., Andica, C., Maekawa, T., Irie, R., Takemura, M.Y., Kumamaru, K.K., Wada, A., Suzuki, M., Ozaki, Y., Abe, O., Aoki, S., 2019. Three-dimensional high-resolution simultaneous quantitative mapping of the whole brain with 3D-QALAS: an accuracy and repeatability study. Magn. Reson. Imaging. https://doi.org/10.1016/j.mri.2019.08.031.

Ganzetti, M., Wenderoth, N., Mantini, D., 2014. Whole brain myelin mapping using T1- and T2-weighted MR imaging data. Front. Hum. Neurosci. 8. https://doi.org/10.3389/fnhum.2014.00671.

Gil, R., Khabipova, D., Zwiers, M., Hilbert, T., Kober, T., Marques, J.P., 2016. An in vivo study of the orientation-dependent and independent components of transverse relaxation rates in white matter. NMR Biomed.. https://doi.org/10.1002/nbm.3616.

Hakkarainen, H., Sierra, A., Mangia, S., Garwood, M., Michaeli, S., Gröhn, O., Liimatainen, T., 2016. MRI relaxation in the presence of fictitious fields correlates with myelin content in normal rat brain. Magn. Reson. Med.. https://doi.org/10.1002/mrm.25590.

Hametner, S., Endmayr, V., Deistung, A., Palmrich, P., Prihoda, M., Haimburger, E., Menard, C., Feng, X., Haider, T., Leisser, M., Köck, U., Kaider, A., Höftberger, R., Robinson, S., Reichenbach, J.R., Lassmann, H., Traxler, H., Trattnig, S., Grabner, G., 2018. The influence of brain iron and myelin on magnetic susceptibility and effective transverse relaxation - A biochemical and histological validation study. Neuroimage. https://doi.org/10.1016/j.neuroimage.2018.06.007.

Harkins, K.D., Valentine, W.M., Gochberg, D.F., Does, M.D., 2013. In-vivo multi-exponential T2, magnetization transfer and quantitative histology in a rat model of intramyelinic edema. NeuroImage Clin. 2, 810–817. https://doi.org/10.1016/j.nicl.2013.06.007.

Heath, F., Hurley, S.A., Johansen-Berg, H., Sampaio-Baptista, C., 2017. Advances in noninvasive myelin imaging. Dev. Neurobiol.. https://doi.org/10.1002/dneu.22552.

Hervé, P.-Y., Cox, E.F., Lotfipour, A.K., Mougin, O.E., Bowtell, R.W., Gowland, P.a, Paus, T., 2011. Structural properties of the corticospinal tract in the human brain: a magnetic resonance imaging study at 7 Tesla. Brain Struct. Funct. 216, 255–262. https://doi.org/10.1007/s00429-011-0306-0.

Janve, V.A., Zu, Z., Yao, S.Y., Li, K., Zhang, F.L., Wilson, K.J., Ou, X., Does, M.D., Subramaniam, S., Gochberg, D.F., 2013. The radial diffusivity and magnetization transfer pool size ratio are sensitive markers for demyelination in a rat model of type III multiple sclerosis (MS) lesions. Neuroimage 74, 298–305. https://doi.org/10.1016/j.neuroimage.2013.02.034.

Jung, W., Lee, Jingu, Shin, H.G., Nam, Y., Zhang, H., Oh, S.H., Lee, Jongho, 2017. Whole brain g-ratio mapping using myelin water imaging (MWI) and neurite orientation dispersion and density imaging (NODDI). Neuroimage.. https://doi.org/10.1016/j.neuroimage.2017.09.053.

Khodanovich, M.Y., Sorokina, I.V., Glazacheva, V.Y., Akulov, A.E., Nemirovich-Danchenko, N.M., Romashchenko, A.V., Tolstikova, T.G., Mustafina, L.R., Yarnykh, V.L., 2017. Histological validation of fast macromolecular proton fraction mapping as a quantitative myelin imaging method in the cuprizone demyelination model. Sci. Rep. 7. https://doi.org/10.1038/srep46686.

Khodanovich, Pishchelko, Glazacheva, Pan, Akulov, Svetlik, Tyumentseva, Anan'ina, Yarnykh, 2019. . Quantitative Imaging of White and Gray Matter Remyelination in the Cuprizone Demyelination Model Using the Macromolecular Proton Fraction. Cells.. https://doi.org/10.3390/cells8101204.

Kolind, S., Seddigh, A., Combes, A., Russell-Schulz, B., Tam, R., Yogendrakumar, V., Deoni, S., Sibtain, N.A., Traboulsee, A., Williams, S.C.R., Barker, G.J., Brex, P.A., 2015. Brain and cord myelin water imaging: a progressive multiple sclerosis biomarker. NeuroImage Clin. 9, 574–580. https://doi.org/10.1016/j.nicl.2015.10.002.

Kozlowski, P., Raj, D., Liu, J., Lam, C., Yung, A.C., Tetzlaff, W., 2008. Characterizing white matter damage in rat spinal cord with quantitative MRI and histology. J. Neurotrauma 25, 653–676. https://doi.org/10.1089/neu.2007.0462.

Laule, C., Kozlowski, P., Leung, E., Li, D.K.B., MacKay, A.L., Moore, G.R.W., 2008. Myelin water imaging of multiple sclerosis at 7 T: correlations with histopathology. Neuroimage 40, 1575–1580. https://doi.org/10.1016/j.neuroimage.2007.12.008.

Laule, C., Leung, E., Li, D.K.B., Traboulsee, A.L., Paty, D.W., MacKay, A.L., Moore, G.R.W., 2006. Myelin water imaging in multiple sclerosis: quantitative correlations with histopathology. Mult. Scler. 12, 747–753. https://doi.org/10.1177/1352458506070928.

Lee, K., Cherel, M., Budin, F., Gilmore, J., Consing, K.Z., Rasmussen, J., Wadhwa, P.D., Entringer, S., Glasser, M.F., Van Essen, D.C., Buss, C., Styner, M., 2015. Early postnatal myelin content estimate of white matter via T1w/T2w ratio. Proc. SPIE–the Int. Soc. Opt. Eng. 9417, 94171R. https://doi.org/10.1117/12.2082198.

Lehto, Lauri J., Albors, A.A., Sierra, A., Tolppanen, L., Eberly, L.E., Mangia, S., Nurmi, A., Michaeli, S., Gröhn, O., 2017a. Lysophosphatidyl choline induced demyelination in rat probed by relaxation along a fictitious field in high rank rotating frame. Front. Neurosci. 11. https://doi.org/10.3389/fnins.2017.00433.

Lehto, Lauri Juhani, Sierra, A., Gröhn, O., 2017b. Magnetization transfer SWIFT MRI consistently detects histologically verified myelin loss in the thalamocortical pathway after a traumatic brain injury in rat. NMR Biomed. 30. https://doi.org/10.1002/nbm.3678.

Levesque, I.R., Chia, C.L.L., Pike, G.B., 2010. Reproducibility of in vivo magnetic resonance imaging-based measurement of myelin water. J. Magn. Reson. Imaging 32, 60–68. https://doi.org/10.1002/jmri.22170.

Lévy, S., Guertin, M.C., Khatibi, A., Mezer, A., Martinu, K., Chen, J.I., Stikov, N., Rainville, P., Cohen-Adad, J., 2018. Test-retest reliability of myelin imaging in the human spinal cord: measurement errors versus region- and aging-induced variations. PLoS One. https://doi.org/10.1371/journal.pone.0189944.

Ljungberg, E., Vavasour, I., Tam, R., Yoo, Y., Rauscher, A., Li, D.K.B., Traboulsee, A., MacKay, A., Kolind, S., 2017. Rapid myelin water imaging in human cervical spinal cord. Magn. Reson. Med.. https://doi.org/10.1002/mrm.26551.

Lodygensky, G.A., Marques, J.P., Maddage, R., Perroud, E., Sizonenko, S.V., Hüppi, P.S., Gruetter, R., 2012. In vivo assessment of myelination by phase imaging at high magnetic field. Neuroimage. https://doi.org/10.1016/j.neuroimage.2011.09.057.

MacKay, A.L., Laule, C., 2016. Magnetic resonance of myelin water: an in vivo marker for Myelin. Brain Plast. 2, 71–91. https://doi.org/10.3233/BPL-160033.

Mangeat, G., Govindarajan, S.T., Mainero, C., Cohen-Adad, J., 2015. Multivariate combination of magnetization transfer, T<inf>2</inf>* and B0 orientation to study the myelo-architecture of the in vivo human cortex. Neuroimage 119, 89–102. https://doi.org/10.1016/j.neuroimage.2015.06.033.

McGrath, T.A., Bossuyt, P.M., Cronin, P., Salameh, J.P., Kraaijpoel, N., Schieda, N., McInnes, M.D.F., 2019. Best practices for MRI systematic reviews and meta-analyses. J. Magn. Reson. Imaging. https://doi.org/10.1002/jmri.26198.

McInnes, M.D.F., Bossuyt, P.M.M., 2015. Pitfalls of systematic reviews and meta-analyses in imaging research[1]. Radiology. https://doi.org/10.1148/radiol.2015142779.

McInnes, M.D.F., Moher, D., Thombs, B.D., McGrath, T.A., Bossuyt, P.M., Clifford, T., Cohen, J.F., Deeks, J.J., Gatsonis, C., Hooft, L., Hunt, H.A., Hyde, C.J., Korevaar, D.A., Leeflang, M.M.G., Macaskill, P., Reitsma, J.B., Rodin, R., Rutjes, A.W.S., Salameh, J.P., Stevens, A., Takwoingi, Y., Tonelli, M., Weeks, L., Whiting, P., Willis, B.H., 2018. Preferred reporting items for a systematic review and meta-analysis of diagnostic test accuracy studies the PRISMA-DTA statement. JAMA - J. Am. Med. Assoc.. https://doi.org/10.1001/jama.2017.19163.

Merkler, D., Boretius, S., Stadelmann, C., Ernsting, T., Michaelis, T., Frahm, J., Brück, W., 2005. Multicontrast MRI of remyelination in the central nervous system. NMR Biomed. 18, 395–403. https://doi.org/10.1002/nbm.972.

Meyers, S.M., Laule, C., Vavasour, I.M., Kolind, S.H., Mädler, B., Tam, R., Traboulsee, A.L., Lee, J., Li, D.K.B., MacKay, A.L., 2009. Reproducibility of myelin water fraction analysis: a comparison of region of interest and voxel-based analysis methods. Magn. Reson. Imaging 27, 1096–1103. https://doi.org/10.1016/j.mri.2009.02.001.

Mottershead, J.P., Schmierer, K., Clemence, M., Thornton, J.S., Scaravilli, F., Barker, G.J., Tofts, P.S., Newcombe, J., Cuzner, M.L., Ordidge, R.J., McDonald, W.I., Miller, D.H., 2003. High field MRI correlates of myelin content and axonal density in multiple sclerosis: a post-mortem study of the spinal cord. J. Neurol. 250, 1293–1301. https://doi.org/10.1007/s00415-003-0192-3.

Nguyen, T.D., Deh, K., Monohan, E., Pandya, S., Spincemaille, P., Raj, A., Wang, Y., Gauthier, S.A., 2016. Feasibility and reproducibility of whole brain myelin water mapping in 4 minutes using fast acquisition with spiral trajectory and adiabatic T2prep (FAST-T2) at 3T. Magn. Reson. Med. 76, 456–465. https://doi.org/10.1002/mrm.25877.

Oh, S.H., Kim, Y.B., Cho, Z.H., Lee, J., 2013. Origin of B0 orientation dependent R2* (=1/T2*) in white matter. Neuroimage.. https://doi.org/10.1016/j.neuroimage.2013.01.051.

Prasloski, T., Mädler, B., Xiang, Q.S., MacKay, A., Jones, C., 2012. Applications of stimulated echo correction to multicomponent T2analysis. Magn. Reson. Med. 67, 1803–1814. https://doi.org/10.1002/mrm.23157.

Ramagopalan, S.V., Dobson, R., Meier, U.C., Giovannoni, G., 2010. Multiple sclerosis: risk factors, prodromes, and potential causal pathways. Lancet Neurol.. https://doi.org/10.1016/S1474-4422(10)70094-6.

Reeves, C., Tachrount, M., Thomas, D., Michalak, Z., Liu, J., Ellis, M., Diehl, B., Miserocchi, A., McEvoy, A.W., Eriksson, S., Yousry, T., Thom, M., 2016. Combined Ex Vivo 9.4T MRI and quantitative histopathological study in normal and pathological neocortical resections in focal epilepsy. Brain Pathol. 26, 319–333. https://doi.org/10.1111/bpa.12298.

Schmierer, K., Scaravilli, F., Altmann, D.R., Barker, G.J., Miller, D.H., 2004. Magnetization transfer ratio and myelin in postmortem multiple sclerosis brain. Ann. Neurol. 56, 407–415. https://doi.org/10.1002/ana.20202.

Schmierer, K., Thavarajah, J.R., An, S.F., Brandner, S., Miller, D.H., Tozer, D.J., 2010. Effects of formalin fixation on magnetic resonance indices in multiple sclerosis cortical gray matter. J. Magn. Reson. Imaging 32, 1054–1060. https://doi.org/10.1002/jmri.22381.

Schmierer, K., Tozer, D.J., Scaravilli, F., Altmann, D.R., Barker, G.J., Tofts, P.S., Miller, D.H., 2007. Quantitative magnetization transfer imaging in postmortem multiple sclerosis brain. J. Magn. Reson. Imaging 26, 41–51. https://doi.org/10.1002/jmri.20984.

Schmierer, K., Wheeler-Kingshott, C.A.M., Tozer, D.J., Boulby, P.A., Parkes, H.G., Yousry, T.A., Scaravilli, F., Barker, G.J., Tofts, P.S., Miller, D.H., 2008. Quantitative magnetic resonance of postmortem multiple sclerosis brain before and after fixation. Magn. Reson. Med. 59, 268–277. https://doi.org/10.1002/mrm.21487.

Shams, Z., Norris, D.G., Marques, J.P., 2019. A comparison of in vivo MRI based cortical myelin mapping using T1w/T2w and R1 mapping at 3T. PLoS One. https://doi.org/10.1371/journal.pone.0218089.

Soustelle, L., Antal, M.C., Lamy, J., Rousseau, F., Armspach, J.P., Loureiro de Sousa, P., 2019. Correlations of quantitative MRI metrics with myelin basic protein (MBP) staining in a murine model of demyelination. NMR Biomed.. https://doi.org/10.1002/nbm.4116.

Tardif, C.L., Bedell, B.J., Eskildsen, S.F., Collins, D.L., Pike, G.B., 2012. Quantitative magnetic resonance imaging of cortical multiple sclerosis pathology. Mult. Scler. Int. 2012, 1–13. https://doi.org/10.1155/2012/742018.

Thiessen, J.D., Zhang, Y., Zhang, H., Wang, L., Buist, R., Del Bigio, M.R., Kong, J., Li, X.M., Martin, M., 2013. Quantitative MRI and ultrastructural examination of the cuprizone mouse model of demyelination. NMR Biomed. 26, 1562–1581. https://doi.org/10.1002/nbm.2992.

Turati, L., Moscatelli, M., Mastropietro, A., Dowell, N.G., Zucca, I., Erbetta, A., Cordiglieri, C., Brenna, G., Bianchi, B., Mantegazza, R., Cercignani, M., Baggi, F., Minati, L., 2015. In vivo quantitative magnetization transfer imaging correlates with histology during de- and remyelination in cuprizone-treated mice. NMR Biomed. 28, 327–337. https://doi.org/10.1002/nbm.3253.

Uddin, M.N., Figley, T.D., Marrie, R.A., Figley, C.R., 2018. Can T1w/T2w ratio be used as a myelin-specific measure in subcortical structures? Comparisons between FSE-based T1w/T2w ratios, GRASE-based T1w/T2w ratios and multi-echo GRASE-based myelin water fractions. NMR Biomed.. https://doi.org/10.1002/nbm.3868.

Ulmer, J.L., Mathews, V.P., Hamilton, C.A., Elster, A.D., Moran, P.R., 1996. Magnetization transfer or spin-lock? An investigation of off-resonance saturation pulse imaging with varying frequency offsets. Am. J. Neuroradiol. 17 (5), 805–819.

Underhill, H.R., Rostomily, R.C., Mikheev, A.M., Yuan, C., Yarnykh, V.L., 2011. Fast bound pool fraction imaging of the in vivo rat brain: association with myelin content and validation in the C6 glioma model. Neuroimage. https://doi.org/10.1016/j.neuroimage.2010.10.065.

Van Der Voorn, J.P., Pouwels, P.J.W., Powers, J.M., Kamphorst, W., Martin, J.J., Troost, D., Spreeuwenberg, M.D., Barkhof, F., Van Der Knaap, M.S., 2011. Correlating quantitative MR imaging with histopathology in X-linked adrenoleukodystrophy. Am. J. Neuroradiol. 32, 481–489. https://doi.org/10.3174/ajnr.A2327.

Varma, G., Girard, O.M., Prevost, V.H., Grant, A.K., Duhamel, G., Alsop, D.C., 2015. Interpretation of magnetization transfer from inhomogeneously broadened lines (ihMT) in tissues as a dipolar order effect within motion restricted molecules. J. Magn. Reson.. https://doi.org/10.1016/j.jmr.2015.08.024.

Warntjes, J.B.M., Persson, A., Berge, J., Zech, W., 2017. Myelin detection using rapid quantitative MR imaging correlated to macroscopically registered luxol fast blue-stained brain specimens. Am. J. Neuroradiol. 38, 1096–1102. https://doi.org/10.3174/ajnr.A5168.

Wayne Moore, G.R., 2003. MRI-clinical correlations: More than inflammation alone-what can MRI contribute to improve the understanding of pathological processes in MS? J. Neurol. Sci.. https://doi.org/10.1016/S0022-510X(02)00347-7.

West, D.J., Teixeira, R.P.A.G., Wood, T.C., Hajnal, J.V., Tournier, J.D., Malik, S.J., 2019. Inherent and unpredictable bias in multi-component DESPOT myelin water fraction estimation. Neuroimage. https://doi.org/10.1016/j.neuroimage.2019.03.049.

West, K.L., Kelm, N.D., Carson, R.P., Gochberg, D.F., Ess, K.C., Does, M.D., 2016. Myelin volume fraction imaging with MRI. Neuroimage. https://doi.org/10.1016/j.neuroimage.2016.12.067.

Whiting, P.F., Rutjes, A.W.S., Westwood, M.E., Mallett, S., Deeks, J.J., Reitsma, J.B., Leeflang, M.M.G., Sterne, J.A.C., Bossuyt, P.M.M., 2011. QUADAS-2: a revised tool for the quality assessment of diagnostic accuracy studies. Ann. Intern. Med. 155, 529–536. https://doi.org/10.7326/0003-4819-155-8-201110180-00009.

Wiggermann, V., Hametner, S., Hernández-Torres, E., Kames, C., Endmayr, V., Kasprian, G., Höftberger, R., Li, D.K.B., Traboulsee, A., Rauscher, A., 2017. Susceptibility-sensitive MRI of multiple sclerosis lesions and the impact of normal-appearing white matter changes. NMR Biomed.. https://doi.org/10.1002/nbm.3727.

Wu, C., Wang, C., Popescu, D.C., Zhu, W., Somoza, E.A., Zhu, J., Condie, A.G., Flask, C.A., Miller, R.H., MacKlin, W., Wang, Y., 2010. A novel PET marker for in vivo quantification of myelination. Bioorganic Med. Chem. 18, 8592–8599. https://doi.org/10.1016/j.bmc.2010.10.018.

Wu, Y., Alexander, A.L., Fleming, J.O., Duncan, I.D., Field, A.S., 2006. Myelin water fraction in human cervical spinal cord in vivo. J. Comput. Assist. Tomogr. 30, 304–306. https://doi.org/10.1097/00004728-200603000-00026.

Zaaraoui, W., Deloire, M., Merle, M., Girard, C., Raffard, G., Biran, M., Inglese, M., Petry, K.G., Gonen, O., Brochet, B., Franconi, J.M., Dousset, V., 2008. Monitoring demyelination and remyelination by magnetization transfer imaging in the mouse brain at 9.4 T. Magn. Reson. Mater. Physics, Biol. Med. 21, 357–362. https://doi.org/10.1007/s10334-008-0141-3.

Zeydan, B., Lowe, V.J., Schwarz, C.G., Przybelski, S.A., Tosakulwong, N., Zuk, S.M., Senjem, M.L., Gunter, J.L., Roberts, R.O., Mielke, M.M., Benarroch, E.E., Rodriguez, M., Machulda, M.M., Lesnick, T.G., Knopman, D.S., Petersen, R.C., Jack, C.R., Kantarci, K., Kantarci, O.H., 2018. Pittsburgh compound-B PET white matter imaging and cognitive function in late multiple sclerosis. Mult. Scler. J.. https://doi.org/10.1177/1352458517707346.

Zhang, J., Kolind, S.H., Laule, C., Mackay, A.L., 2015. Comparison of myelin water fraction from multiecho T2 decay curve and steady-state methods. Magn. Reson. Med. 73, 223–232. https://doi.org/10.1002/mrm.25125.

Zhang, L., Chen, T., Tian, H., Xue, H., Ren, H., Li, L., Fan, Q., Wen, B., Ren, Z., 2019. Reproducibility of inhomogeneous magnetization transfer (ihMT): a test-retest, multi-site study. Magn. Reson. Imaging. https://doi.org/10.1016/j.mri.2018.11.010.